ARTICLE

ACS chemical biology

Anticonvulsant Met-Enkephalin Analogues Containing Backbone Spacers Reveal Alternative Non-Opioid Signaling in the Brain

Hee-Kyoung Lee[†,#], Misty D. Smith[‡,#], Brian J. Smith[§], Joel Grussendorf[‡], Liping Xu[∥,⊥], Robert J. Gillies[∥,⊥], H. Steve White[‡], and Grzegorz Bulaj[†,*]

[†]Department of Medicinal Chemistry, and [‡]Department of Pharmacology and Toxicology, The University of Utah, 421 Wakara Way, Suite 360, Salt Lake City, Utah 84108, [§]The Walter and Eliza Hall Institute of Medical Research, Parkville 3052, Australia, [∥]Department of Radiology, and [⊥]Department of Biochemistry and Molecular Biophysics, Arizona Health Sciences Center, University of Arizona, Tucson, Arizona 85724. #These authors contributed equally to this work.

ABSTRACT Prosthesis of non-critical parts of a polypeptide backbone is an attractive strategy to simplify bioactive peptides. This approach was applied to an opioid neuropeptide, Met-enkephalin, in which two adjacent Gly2-Gly3 residues were replaced with a series of non-peptidic backbone spacers varying in length and/or physicochemical properties. The backbone spacers did not affect the overall structural properties of the analogues, but they did dramatically reduce their affinities and agonist activities toward δ- and μ-opioid receptors. Molecular modeling suggested that the decrease of the affinity of Met-enkephalin to δ-opioid receptor could be accounted for by the loss of a single hydrogen bond. Remarkably, the analogues containing the most isostere spacers retained potent antinociceptive and anticonvulsant properties that were comparable to that of the endogenous peptide. This unexpected high *in vivo* potency could not be accounted for by an increase in metabolic stability. Moreover, the antiepileptic activity could not be reversed by opioid receptor antagonists. In summary, the results obtained with the analogues containing backbone spacers suggest a novel mechanism for seizure control in the brain that involves alternative non-opioid signaling.

To transform peptides into therapeutics, numerous drug design strategies have been developed. In addition to various peptidomimetic approaches (*1, 2*), chemical modifications of peptides are effective in improving their bioavailability and pharmaceutical properties. Successful chemical modifications include cyclization, lipidization, glycosylation, cationization, or PEGylation, among others. In an attempt to modify a peptide backbone, two approaches have been employed: the replacement of a peptide bond with a stable pseudopeptide bond (*3*) or the replacement of adjacent amino acid residues with non-natural modules, such as oligomer-β-acids (*4*) or non-natural amino acids (*5*). The growing body of structural studies on peptidomimetics containing α-, β-, γ-, and δ-amino acid residues suggests that backbone modification vastly expands the repertoire of peptide structure and function (*6, 7*).

Backbone prosthesis is a drug design strategy in which non-essential amino acid residues are replaced with isostere non-peptidic backbone spacers (*8*). Recently, this approach was successfully employed to improve the pharmacological properties of conotoxins. For example, replacing adjacent amino acid residues with non-natural spacers, such as 5-amino-3-oxapentanoic acid or 6-aminohexanoic acid, resulted in analogues that were better blockers of sodium channels and more potent, longer lasting analgesics (*8*). This strategy has also been applied to other peptides such as neuropeptide Y (NPY) (*9*), calcitonin (*10*), tyrocidines (*11*), and glucagon-like-peptide-1 (GLP-1) (*12*). The size-reduced NPY showed high affinity for its receptor (*9*). The substi-

***Corresponding author,** bulaj@pharm.utah.edu.

Received for review June 4, 2008 and accepted June 30, 2009.

Published online June 30, 2009

10.1021/cb900045c CCC: $40.75

tutions in the α-helical region in calcitonin with a linear ethylene glycol resulted in analogues showing significant affinity for its target receptor (*10*). The modified tyrocidines with a flexible spacer showed a turnover rate for peptide synthetase that was comparable to that of its natural substrate (*11*). The insertion of 6-aminohexanoic acid in GLP-1 produced an effective and long-lasting GLP-1 analogue (*12*). Since more and more structure−activity relationship (SAR) studies on various peptides of therapeutic potential are available, the backbone prosthesis is likely to be more often employed to modify the pharmacological and pharmaceutical properties of peptides.

In this study, we explored the backbone prosthesis strategy with the endogenous opioid neuropeptide Met-enkephalin (YGGFM), which binds with high affinity to δ-opioid receptors (δOR) and to a lesser extent to μ-opioid receptors (μOR). Opioid peptides have been a workhorse for peptide engineering and the development of peptide-based therapeutics (*13–16*). To improve the bioavailability of these peptides, numerous approaches including cyclization (*17, 18*), glycosylation (*19–22*), and backbone modifications (*23*) have been reported. To test the backbone prosthesis approach with the peptide Met-enkephalin, we replaced the adjacent Gly2-Gly3 motif with backbone spacers varying in length and/or physicochemical properties. Based on unique properties observed with the backbone spacer-containing analogues, we report two unexpected findings. First, a single peptide bond between Gly2 and Gly3 is critical for maintaining high-affinity at the opioid receptors. Second, since naloxone (nonselective opioid receptor antagonist) and naloxonazine (μOR-specific antagonist) did not reverse the anticonvulsant activity of the low-affinity Met-enkephalin analogues containing backbone spacers, our results suggest that endogenous opioid peptides may control seizures *via* alternative non-opioid pathways in the brain. In general, insights gleaned from the backbone prosthesis approach may lead to the development of novel peptide-based pharmacological tools and therapeutic strategies for the treatment of epilepsy, pain, and other neurological disorders.

RESULTS AND DISCUSSION

To study structural and functional consequences of the backbone prosthesis applied to neuroactive peptides, five Met-enkephalin analogues were designed in which the adjacent Gly2-Gly3 residues were replaced with the backbone spacers, such as a PEG-spacer (5-amino-3-oxapentanoic acid) or a series of extended glycine amino acids: 4-aminobutyric acid, 5-aminopentanoic acid, 6-aminohexanoic acid, or 7-aminoheptanoic acid (Figure 1). These analogues were investigated using molecular dynamics (MD) simulations and were chemically synthesized to assess their functional properties. Using an automated peptide synthesizer and *N*-(9-fluorenyl) methoxycarbonyl (Fmoc) chemistry, the analogues were assembled, removed from the resin, and purified by reversed-phase HPLC (RP-HPLC). The chemical identity of the analogues was confirmed by MALDI-TOF mass spectrometry (Supplementary Table S1).

Molecular Modeling. To explore structural consequences of replacing the Gly2-Gly3 sequence by the backbone spacers varying in length, we calculated a distance between aromatic rings of Tyr1 and Phe4 for the analogues (Figure 1). The MD calculations on Met-enkephalin showed the lack of a preferred structure in aqueous solution (also independently confirmed by our NMR studies; data not shown). At no time during the MD trajectory was the geometry consistent with the formation of hydrogen bonds between any of the backbone atoms of Tyr1 and Phe4, in contradiction to early NMR studies in D_2O (*24*). The formation of a salt bridge between the amino terminal group and carboxyl terminal group was observed transiently throughout the simulation, accounting for ~10% of the structural population. Secondary-structure analysis also indicated the transient formation of a turn structure that accounted for ~15% of the structural population. These results are similar to earlier MD studies of Leu-enkephalin in water (*25*).

The MD simulations indicate that there is no preferred structure among the backbone-spacer analogues. Consistent with a lack of structure, we observed no sustained contact between the side chains of the Tyr1 and Phe4 of any of the Met-enkephalin analogues during the 100 ns MD simulation. The distance between the centroids of the aromatic rings of these residues was calculated on the basis of the MD simulations (Supplementary Figure S1). The mean distance and standard deviation for each analogue are presented in Figure 1. The large mean separation (10−12 Å) and large variation in the observed separation (standard deviation ~3 Å) highlights the transient nature of the contact between

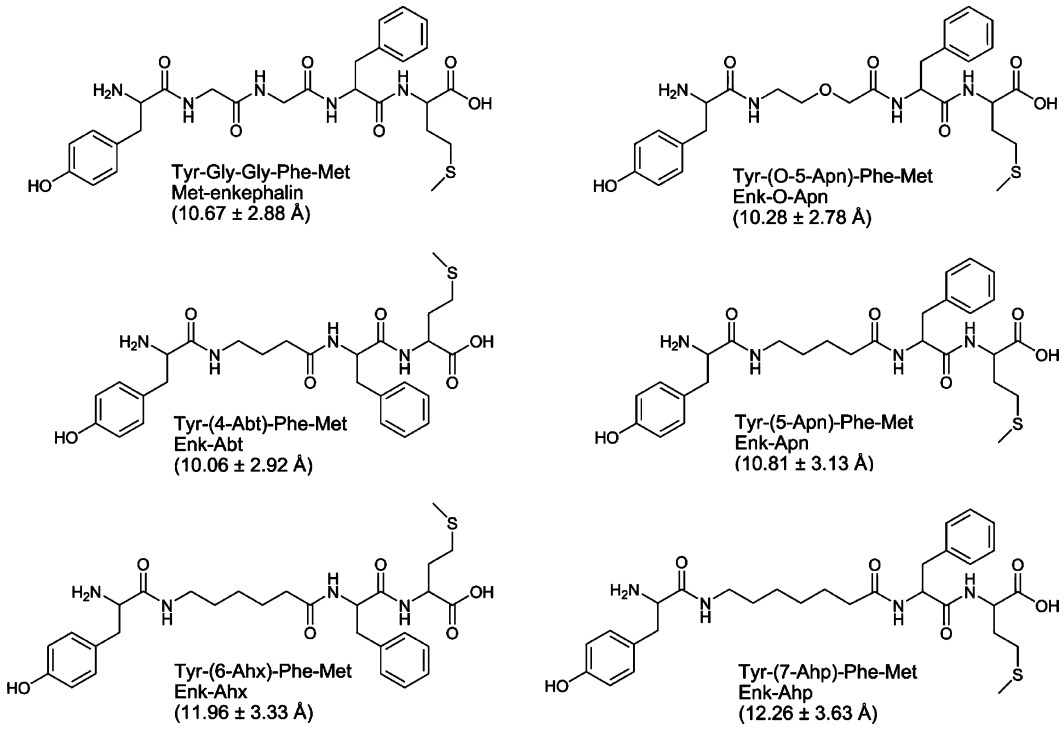

Figure 1. Design of Met-enkephalin analogues containing backbone spacers. The adjacent Gly2-Gly3 residues were replaced with selected backbone spacers (O-5-Apn, 5-amino-3-oxapentanoic acid; 4-Abt, 4-aminobutyric acid; 5-Apn, 5-aminopentanoic acid; 6-Ahx, 6-aminohexanoic acid; 7-Ahp, 7-aminoheptanoic acid). The values in parentheses are the distance between the centroids of the aromatic rings of Tyr1 and Phe4 in Met-enkephalin and the analogues calculated from MD simulations.

the two aromatic rings. As predicted, longer spacers resulted in larger distances between Tyr1 and Phe4.

Receptor Binding Studies. The receptor binding of all analogues was tested with europium-labeled [D-Pen2, L-Cys5] enkephalin (DPLCE) using CHO cells overexpressing the human δOR (*26*). The cyclized analogue, DPLCE, was shown to have high potency for peripheral δOR (*18*). The binding affinity of the selected analogues for μOR and κ-opioid receptor (κOR) was determined using [^{3}H]diprenorphine and [^{3}H]U-69593, respectively. The replacement of the Gly2-Gly3 sequence with the backbone spacers dramatically reduced the ability of the analogues to bind to the opioid receptors (Table 1). The affinity of all analogues for the δOR was decreased by 4 orders of magnitude as compared to Met-enkephalin. Similarly, the affinity for μOR was reduced by 2 orders of magnitude for the Met-enkephalin analogue with the Gly2-Gly3 residues replaced by 5-amino-3-oxapentanoic acid (Enk-O-Apn) and more than 3 orders of magnitude for the Met-enkephalin analogue with the Gly2-Gly3 residues replaced by 5-aminopentanoic acid (Enk-Apn). Met-enkephalin and two selected analogues were also studied for potential interactions with κOR, which is known to mediate anticonvulsant activity of dynorphin, another endogenous opioid peptide (*27*). As shown in Table 1, neither Met-enkephalin nor the analogues displaced [^{3}H]U-69593 at a concentration of 10 μM. Our receptor binding data are consistent with a previous study with the Leu-enkephalin analogue in which the amide linkages between Gly2-Gly3 were replaced by ketomethylene groups (*28*). The resulting analogue had 1/4000 and 1/2400 the opioid receptor binding activity of Leu-enkephalin when [^{3}H][D-Ala2, D-Leu5] enkephalin and [^{3}H]naloxone, respectively, were used as tritiated ligands (Table 2). A similar approach of incorporating of 4-aminocyclohexylcarboxylic acid into the peptide backbone of dynorphin A (*29*) or 1,5-enediols into the pep-

TABLE 1. Binding affinity and anticonvulsant activity of Met-enkephalin analogues[a]

	In vitro assays (receptor binding)			*In vivo* assay (anticonvulsant, icv)
Analogue	**δOR K_i [nM]**	**μOR K_i [nM]**	**κOR K_i [nM]**	**ED_{50} (95% CI) (nmol)**
Y-GG-FM	4	19	>10,000	0.91 (0.69−1.41)
Y-(O-5-Apn)-FM	30,000	1,300	>10,000	0.83 (0.28−1.66)
Y-(4-Abt)-FM	86,000	n.d.	n.d.	>2
Y-(5-Apn)-FM	48,000	>10,000	n.d.	1.71 (0.95−2.99)
Y-(6-Ahx)-FM	40,000	>10,000	>10,000	0.47 (0.14−1.15)
Y-(7-Ahp)-FM	19,000	n.d.	n.d.	>6

[a]The binding assay for δOR was carried out in a CHO cell line using Eu-labeled-DPLCE. The binding assays for μOR were conducted in a CHO cell line using [^{3}H]diprenorphine. The binding assay for κOR was carried out in guinea pig cerebellar membranes using [^{3}H]U-69593. Anticonvulsant potency of the Met-enkephalin analogues was determined in the 6 Hz mouse model of epilepsy following icv administration.

tide backbone of endomorphin (*30*) has been described; unlike our analogues, however, those analogues showed either modest or high affinity to κOR or μOR, respectively.

Our receptor binding studies suggest an unprecedented contribution of a single peptide bond to the interactions between opioid peptides and their receptors. It is not easy to interpret this unexpected finding at a structural level, since no details of molecular interactions are available from the literature. Therefore, in order to map interactions between the Gly2-Gly3 of Met-enkephalin and δOR, a molecular model of the receptor was constructed using the structure of the β_2 adrenergic G protein-coupled receptor (GPCR) as a template (*31*), followed by docking experiments. The highest ranked docking prediction of Met-enkephalin with the δOR is presented in Figure 2. Many of the high-ranking predictions placed the hydroxyl group of Tyr1 hydrogen-bonded to D95 close to the center of the receptor (this amino acid residue is highly conserved among GPCRs), which corresponds with the region comprising the group-3 amino acids identified by Décaillot et al. (*32*). The carboxy terminal of the ligand is located toward the extracellular region of δOR, exposed to solvent and forming a salt bridge with K108. The side chain of Met5 is predicted to lie in close proximity to W284, V296, and V297, shown to be important for binding of δOR-selective ligands (*33*). The side chain of Phe4 packs against Y129, also implicated in the binding of ligands (*34*). The Gly2-Gly3 N−H amides form hydrogen bond interactions with D128 and Y308. Were the Enk-O-Apn to bind the receptor in a similar manner as predicted

TABLE 2. Functional consequences of the removal of a peptide bond in enkephalin analogues

	Met-enk	**Enk-O-Apn**	**Leu-enk[a]**	**Ketomethylene-Leu-enk[a]**
Backbone linkage	-NH-CH_2-**CO-NH**-CH_2-CO-	-NH-CH_2-**CH_2-O**-CH_2-CO-	-**NH-CH_2-CO-NH**-CH_2-CO-	-**CH_2-CH_2-CO-CH_2**-CH_2-CO-
Distance	10.67 Å[b]	10.28 Å[b]	n.d.	n.d.
Binding affinity	4 nM[c]	30,000 nM[c]	8.4 nM[d]	33,000 nM[d]
Metabolic stability[e]	4.3 min	18.6 min	n.d.	n.d.
Analgesia	43.4% (at 1 nmol)[f]	32.9% (at 1 nmol)[f]	ED_{50} = 240 μg[g]	ED_{50} = 24.3 μg[g]
Anticonvulsant activity	ED_{50} = 0.91 nmol[h]	ED_{50} = 0.83 nmol[h]	n.d.	n.d.

[a]Data for Leu-enk and Ketomethylene-Leu-enk were taken from Almquist *et al.* (*28*). [b]Distance between the centroids of the aromatic rings of Tyr1 and Phe4 calculated from MD simulations. [c]K_i values for binding to δOR from our studies. [d]IC_{50} values for binding to the opioid receptors from rat brain membranes using radiolabeled DADLE. [e]Metabolic stability was measured using rat serum. [f]Analgesic (inflammatory) response in formalin test after icv administration. [g]Analgesic response in the tail flick assay after icv administration. The converted ED_{50}'s for Leu-enk and Ketomethylene-Leu-enk are 430 and 44 nmol, respectively. [h]ED_{50} was determined in the 6 Hz partial psychomotor seizure model.

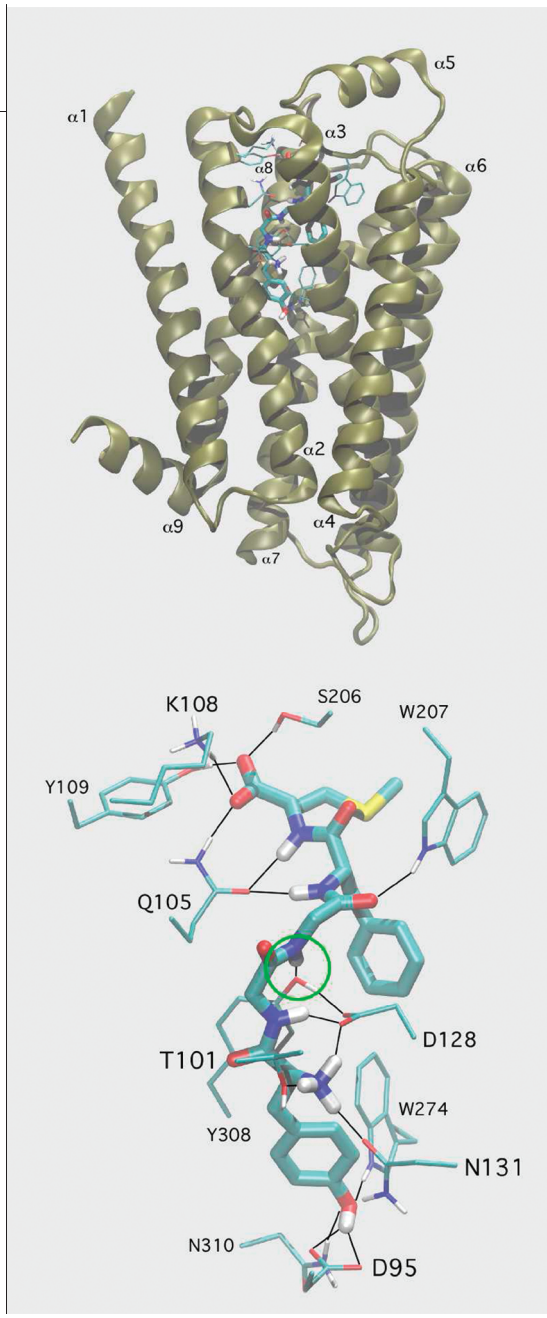

Figure 2. Molecular model of Met-enkephalin bound to δOR. Top) Ribbon diagram of δOR with Met-enkephalin bound. Bottom) Interactions of Met-enkephalin (thick rods) with the residues in δOR (thin rods). Hydrogen bonds are indicated by black lines. The top-scoring conformation from the docking simulations places the hydroxyl group of Tyr1 close to the center of δOR, hydrogen-bonded to D95, a highly conserved amino acid residue among GPCRs. The charged amino terminal of Met-enkephalin forms a salt bridge with D128, a highly conserved residue among opioid receptors. The hydrogen bond between the hydroxyl group of Y308 and the backbone amide of Gly3 is circled in green; this interaction would be missing in the interaction of Enk-O-Apn and is proposed to contribute to the drastic decrease in the affinity toward δOR.

here for Met-enkephalin, the single hydrogen bond between the N−H amide of Gly3 and the hydroxyl group of Y308 would be lost. Several models of δOR, including complexes with a variety of ligands, have been reported (*34–36*). All previous models placed the N-terminal ammonium of the ligand in close proximity to the highly conserved residue D128. Hydrogen bonding between D128 and Y308 has been postulated to tether the transmembrane domain 3 (TM3) and transmembrane domain 7 (TM7) in the inactive conformation of the receptor (*36*); these interactions are preserved in our model. In the earlier model, the hydroxyl group of the Y129 side chain is known to contribute to ligand binding (*34*). In our model, this OH group is tethered to W209 and maintains the hydrophobic pocket into which Phe4 of the ligand binds. However, in our model, the ligand is predicted to bind significantly more deeply into the δOR, with the hydroxyl of Tyr1 of Met-enkephalin hydrogen-bonded to residues D95, N310, and W274 in δOR.

Intracellular Calcium Mobilization Assay. The ability of the analogues to stimulate δOR- or μOR-mediated Ca^{2+} mobilization was tested in HEK-293T cells co-expressed with chimeric G proteins. As shown in Figure 3, the activation of intracellular Ca^{2+} mobilization by Met-enkephalin was dose-dependent with EC_{50} values of 3.4 and 53.1 nM for δOR and μOR, respectively. However, the activation of intracellular Ca^{2+} mobilization by Enk-O-Apn exhibited no response for δOR up to a concentration of 10 μM, which is consistent with a substantial loss of affinity toward δOR. The activation of intracellular Ca^{2+} mobilization for μOR was significantly compromised; the EC_{50} values for μOR were estimated to be greater than 10 μM, which is in accord with substantially decreased binding affinity for μOR (K_i = 1.3 μM). Similar correlations between binding and agonist activities were previously observed for nociceptin/dynorphin chimeric peptides with the opioid receptor-like 1 (ORL1) receptor and κOR (*37*), and for a series of dynorphin A analogues toward κOR (*38*).

Anticonvulsant Activity. Met-enkephalin and other opioid peptides have been reported to alter the hippocampal plasticity (*39*). As such, it was suggested to play an anticonvulsant role in the seizure-susceptible El mouse (*40*). Conversely, one report suggested that enkephalin might possess proconvulsant activity; for example, in unrestrained rats Met-enkephalin was reported to produce electroencephalographic (EEG) seizure (*41*). Furthermore, low-affinity analogues of Leu-

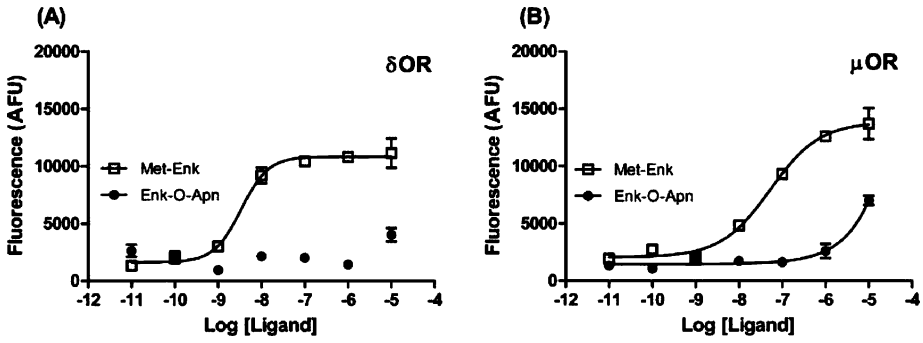

Figure 3. Calcium mobilization assay for δOR (A) and μOR (B). Met-enkephalin (□) produced a concentration-dependent activation of Ca^{2+} with EC_{50} values of 3.4 and 53.1 nM for δOR and μOR, respectively. In contrast, Enk-O-Apn (●) did not affect intracellular Ca^{2+} mobilization mediated by δOR. The EC_{50} for Enk-O-Apn for μOR was estimated to be higher than 10 μM.

enkephalin can retain high *in vivo* potency; the replacement of the peptide bond between Gly2-Gly3 with ketomethylene groups did not significantly affect their analgesic potency despite a 4 orders of magnitude loss in binding affinity (*28*). Thus, despite the dramatic decrease in the affinity of our backbone spacer-containing analogues toward the opioid receptors, we continued to investigate their *in vivo* efficacy in both a mouse model of pain and a mouse model of epilepsy following intracerebroventricular (icv) administration. All of the analogues were evaluated in adult male CF-1 mice in the low frequency (6 Hz) and long duration (3 s) partial psychomotor seizure model; the 6 Hz partial psychomotor seizure model has been shown to be a valuable tool in identifying compounds with unique anticonvulsant profiles (*42–44*). Corneal stimulation in this paradigm produces seizure activity characterized by stereotypic jaw and forelimb clonus, immobility, and an elevated Straub tail (*45*). Mice not demonstrating these behaviors following corneal stimulation are considered protected. Our results in the current study suggest that Met-enkephalin is a potent anticonvulsant with an ED_{50} value of 0.91 nmol (Table 1, Supplementary Table S2). Interestingly, three analogues containing backbone spacers exhibited anticonvulsant potency comparable to that of Met-enkephalin (Table 1). The introduction of a short (4-aminobutyric acid) or long (7-aminoheptanoic acid) spacer resulted in analogues with greater than 2-fold reduction in potency. The nanomolar potency of Met-enkephalin and these analogues in the 6 Hz test is noteworthy given that some marketed antiepileptic drugs lose their efficacy in this model of pharmacoresistant epilepsy (*45, 46*). Moreover, Met-enkephalin (2 nmol) produced minimal rotorod impairment: 3 of 8 mice displayed impaired rotorod performance. In contrast, Enk-O-Apn produced no rotorod impairment, even at the highest dose evaluated (4 nmol). Rotorod performance was measured by placing individual mice on a knurled rotating rod (2.5 cm diameter, 6 rpm). At each concentration tested, eight mice were dosed with the analogue (icv) and examined for minimal motor deficits on the rotorod device 30 min later.

To test whether the anticonvulsant actions of Met-enkephalin and Enk-O-Apn were mediated *via* the opioid signaling pathways, we examined their activities in the presence of either naloxone (nonselective opioid receptor antagonist) or naloxonazine (μOR-selective antagonist). The anticonvulsant activity of both Met-enkephalin and Enk-O-Apn was *not* reversed by systemically administered naloxone (Table 3). Mice were treated with 5 mg kg^{-1} of naloxone or 0.9% saline intraperitoneal (ip). At the time of peak effect (TPE) of naloxone (30 min), they were treated with Met-enkephalin or Enk-O-Apn (2 nmol, 5 μL, icv). Thirty minutes later, animals were challenged with corneal stimulation (6 Hz, 32 mA, 3 s). In the saline-treated group, 4 out of 8 mice were protected by Met-enkephalin or Enk-O-Apn. In the naloxone-treated group, 5 out of 8 mice

TABLE 3. Reversal of anticonvulsant activity of Met-enkephalin and Enk-O-Apn[a]

	Percent of protected mice	
Treatment	**Met-enk**	**Enk-O-Apn**
Saline	50	50
Naloxone	63	50
Naloxonazine	75	75

[a]Mice were pretreated with saline, naloxone, or naloxonazine. At the TPE of each antagonist, mice received either Met-enkephalin or Enk-O-Apn (2 nmol, 5 μL, icv). Thirty minutes later, mice were challenged with corneal stimulation (6 Hz, 32 mA, 3 s). The percent of protected mice in each experimental group (from a total of $n = 8$) is reported.

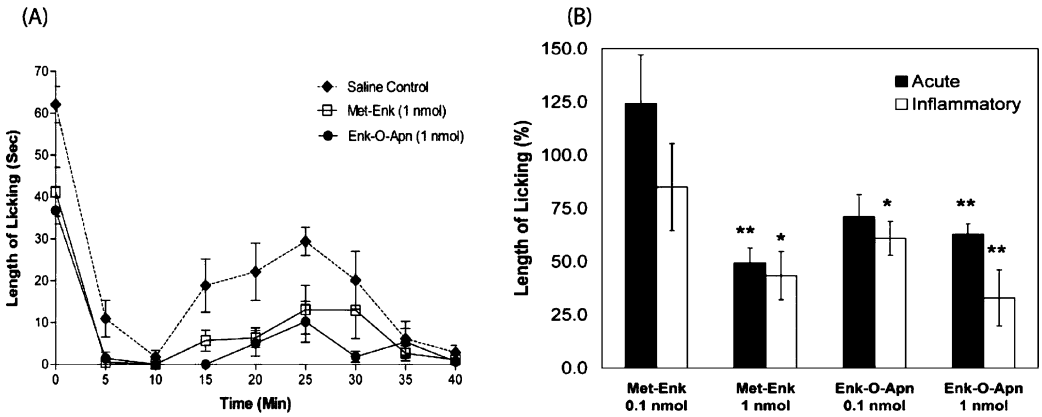

Figure 4. Time–response (A) and dose–response (B) for formalin-induced hyperalgesia. Fifteen minutes after icv administration of either Met-enkephalin or Enk-O-Apn, formalin was injected into the plantar region of one hind paw. A) Results are expressed as the length of licking for both the phase I (acute) and the phase II (inflammatory) responses. Both Met-enkephalin (1 nmol) and Enk-O-Apn (1 nmol) produced a marked reduction in the phase II response. A reduction in the phase I response was also noted for both compounds. B) Results are expressed as a percentage of that observed in the untreated control animals. Both Met-enkephalin and Enk-O-Apn displayed a dose-dependent reduction in the phase II response. The phase II response to Met-enkephalin was decreased as the dose was increased from 0.1 to 1 nmol (85.0 ± 20.4% to 43.4 ± 11.4%, $p < 0.05$). Similarly, the phase II response to Enk-O-Apn was decreased (60.9 ± 7.9%, $p < 0.01$ to 32.9 ± 13.2%, $p < 0.05$). Met-enkephalin was also effective in reducing the phase I response in a dose-dependent manner (124.0 ± 23.0% to 49.3 ± 7.0%, $p < 0.01$), whereas Enk-O-Apn did not exert any significant effect (71.0 ± 10.4% to 62.8 ± 5.0%, $p < 0.01$).

were protected by Met-enkephalin, whereas 4 out of 8 mice were protected by Enk-O-Apn. Similarly, naloxonazine administration (35 mg kg^{-1}, subcutaneous (sc)) did *not* reverse the anticonvulsant activity of Met-enkephalin and Enk-O-Apn (Table 3). At the TPE of naloxonazine (24 h), mice were treated with either Met-enkephalin or Enk-O-Apn. Thirty minutes later, animals were challenged with corneal stimulation. In the saline-treated group, 4 out of 8 mice were protected by Met-enkephalin or Enk-O-Apn. In the naloxonazine-treated group, 6 out of 8 mice were protected by Met-enkephalin or Enk-O-Apn. These reversal experiments strongly suggest that Met-enkephalin exerts its anticonvulsant action *via* a non-opioid mechanism of action. To this point, it is worth emphasizing the discrepancy between their high *in vivo* potency and their low affinity at the opioid receptor. This, coupled with the inability of both antagonists (naloxone and naloxonazine) to reverse the anticonvulsant action of the analogues, suggests an alternative signaling pathway for both Met-enkephalin and Enk-O-Apn. Obviously, the anticonvulsant action of these two opioid analogues could be mediated by off-target activity through a yet undefined mechanism. However, it is important to note that the analgesic effects of both Met-enkephalin and Enk-O-Apn are completely reversed by naloxone (see below).

Antinociceptive Assay. The analgesic activity of Met-enkephalin and Enk-O-Apn was tested in the mouse formalin test. When injected into one of the hind-paws, formalin produces allodynia and inflammation. For this test, vehicle (0.9% saline) or one of the peptide analogues was administered in a total volume of 5 μL, 15 min prior to being challenged with an intraplantar injection of 5% formalin. The injection of formalin induces a characteristic biphasic licking response that can be reduced by analgesic compounds. As summarized in Figure 4, panel A, 1 nmol of Met-enkephalin reduced the phase I (acute) response to 49.3 ± 7.0% ($p < 0.01$) of control. In addition, the phase II (inflammatory) response was reduced to 43.4 ± 11.4% ($p < 0.05$) of control. For the same dose of Enk-O-Apn, the phase I response was reduced to 62.8 ± 5.0% ($p < 0.01$), whereas phase II response was reduced to 32.9 ± 13.2% ($p < 0.01$). As shown in Figure 4, panel B, both compounds displayed a dose-dependent reduction in the phase II response. The phase II response to Met-enkephalin was decreased from 85.0 ± 20.4% to 43.4

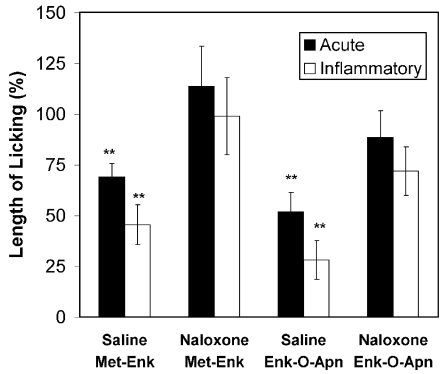

Figure 5. Reversal of analgesic activity by naloxone. Mice were pretreated with 5 mg kg^{-1} of naloxone or saline (ip) 30 min prior to Met-enkephalin or Enk-O-Apn (2 nmol, 5 μL, icv). Naloxone treatment reversed the analgesic efficacy of both Met-enkephalin and Enk-O-Apn. The phase I response to Met-enkephalin was reversed by naloxone treatment (69.0 ± 6.7% to 113.8 ± 19.8%, $p < 0.01$), and the phase II response was also reversed (45.5 ± 9.8% to 99.0 ± 18.9%, $p < 0.01$). Similarly, the phase I response to Enk-O-Apn was reversed by naloxone treatment (51.8 ± 13.2% to 88.4 ± 13.2%, $p < 0.01$), and the phase II response was also reversed (28.1 ± 9.5% to 71.9 ± 12.1%, $p < 0.01$).

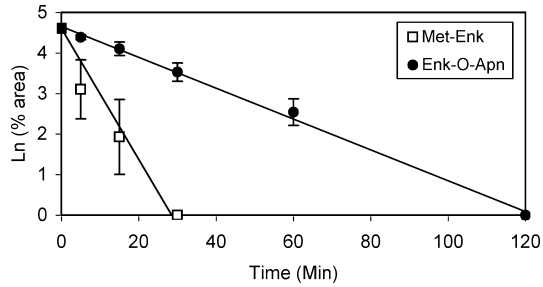

Figure 6. Comparison of the metabolic stability of Met-enkephalin (□) and Enk-O-Apn (●). Incubation of peptides was carried out in 20% rat serum at 37 °C for varying duration of time. The concentration of each peptide was determined by RP-HPLC. The calculated half-life for Met-enkephalin and Enk-O-Apn was determined to be 4.3 and 18.6 min, respectively.

± 11.4% ($p < 0.05$) as the concentration was increased from 0.1 to 1 nmol, whereas the phase II response to Enk-O-Apn decreased from 60.9 ± 7.9% ($p < 0.05$) to 32.9 ± 13.2% ($p < 0.01$). In the phase I response, Met-enkephalin was also effective in a dose-dependent manner (from 124.0 ± 23.0% to 49.3 ± 7.0%, $p < 0.01$). In contrast, Enk-O-Apn did not significantly decrease the phase I response as the dose was increased (71.0 ± 10.4% to 62.8 ± 5.0%, $p < 0.01$). It is also noteworthy to mention that Met-enkephalin was equally efficacious when delivered systemically. At a dose of 4 mg kg^{-1}, Met-enkephalin produced a significant reduction in both phase I (64.3 ± 6.4%, $p < 0.05$) and phase II (29.6 ± 7.0%, $p < 0.01$) responses 15 min after ip administration (results not shown). Similarly, at the same dose, Enk-O-Apn also produced a significant reduction in both phase I (67.5 ± 3.6%, $p < 0.05$) and phase II (30.9 ± 16.9%, $p < 0.01$) responses (results not shown).

In contrast to the anticonvulsant activity, the antinociceptive activity of Met-enkephalin and Enk-O-Apn was reversed by naloxone (non-selective opioid receptor antagonist) (Figure 5). Following the administration of 5 mg kg^{-1} naloxone (ip), the phase I response to Met-enkephalin was reversed to 113.8 ± 19.8% (as compared to 69.0 ± 6.7%, $p < 0.01$ for the saline/Met-enkephalin treatment group); in addition, the phase II response was reversed to 99.0 ± 18.9% (as compared to 45.5 ± 9.8%, $p < 0.01$ for the saline/Met-enkephalin treatment group). With the same dose of naloxone (ip), the phase I response to Enk-O-Apn was reversed to 88.4 ± 13.2%, (as compared to 51.8 ± 13.2%, $p < 0.01$ for the saline/Enk-O-Apn treatment group). The phase II response was reversed to 71.9 ± 12.1% (as compared to 28.1 ± 9.5%, $p < 0.01$ for the saline/Enk-O-Apn treatment group). Meanwhile, the antinociceptive activity of Met-enkephalin and Enk-O-Apn was not reversed by naloxonazine (μOR-selective antagonist). Following the administration of 35 mg kg^{-1} naloxonazine (sc), the phase I response to Met-enkephalin was 66.9 ± 7.4%, $p < 0.05$ (as compared to 48.5 ± 6.6%, $p < 0.01$ for the saline/Met-enkephalin treatment group). The phase II response was 9.5 ± 5.2%, $p < 0.01$ (as compared to 41.5 ± 12.7%, $p < 0.01$ for the saline/Met-enkephalin treatment group). With the same dose of naloxonazine (sc), the phase I response to Enk-O-Apn was 48.1 ± 8.5%, $p < 0.01$ (as compared to 31.1 ± 6.1%, $p < 0.01$ for the saline/Enk-O-Apn treatment group). The phase II response was 4.6 ± 2.5%, $p < 0.01$ (as compared to 11.8 ± 4.4%, $p < 0.01$ for the saline/Enk-O-Apn treatment group). Our results from these reversal experiments suggest that the analgesic activity of Met-enkephalin and Enk-O-Apn are not due to μOR activation but due to δOR activation. Although the analgesic activity of Met-enkephalin could simply be accounted for by the direct agonist activity, we cannot rule out a

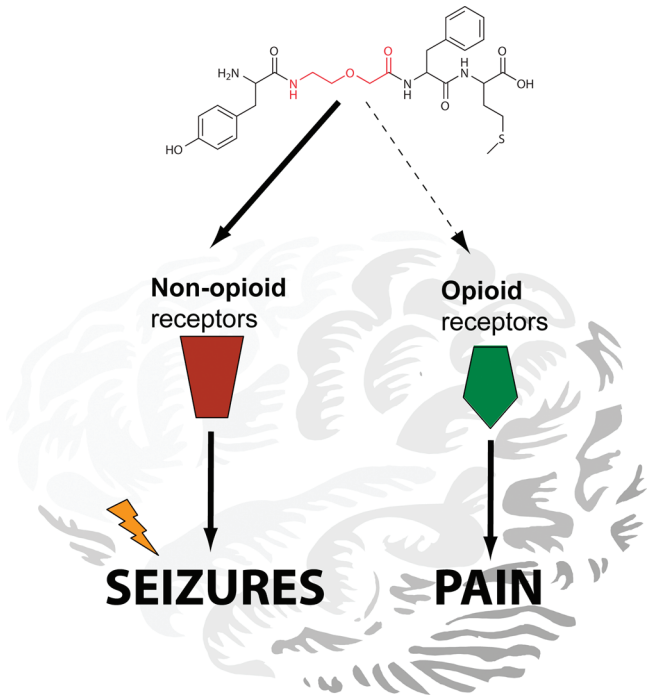

Figure 7. Proposed mechanism for controlling seizures in the brain by Met-enkephalin and its analogues containing selected backbone spacers. Endogenous Met-enkephalin controls pain sensation *via* opioid receptors; however, on the basis of the lack of reversal by either naloxone or naloxonazine, its anticonvulsant effects are likely mediated by non-opioid receptors. The Enk-O-Apn shown here can still control seizures and pain, despite losing activity at opioid receptors (in particular δOR, but also μOR). The potent antiepileptic activity of Enk-O-Apn was not reversed by non-selective or μOR-selective antagonists of opioid receptors, revealing an alternative, non-opioid signaling pathway in the brain that can suppress seizures.

possibility that Enk-O-Apn might produce analgesia by modulating the release of endogenous opioid peptides (that also contribute to the antinociception as reported elsewhere (*47, 48*)).

Metabolic Stability. Since the dramatic differences observed between the *in vitro* and *in vivo* potencies of the analogues could be accounted for by a significant increase in metabolic stability, we compared the half-life of Met-enkephalin and Enk-O-Apn in a serum stability assay. Both peptides were incubated in 20% rat serum at 37 °C, and the amount of remaining intact peptide was quantified by RP-HPLC. As shown in Figure 6, the metabolic stability of Enk-O-Apn was improved ($t_{1/2}$ = 18.6 min) as compared to Met-enkephalin ($t_{1/2}$ = 4.3 min). However, this several-fold increase in the metabolic stability could not explain the discrepancies between the receptor binding affinity and the *in vivo* potency, as previously suggested (*28*). The increased metabolic stability of Enk-O-Apn does, however, suggest that this analogue may be less susceptible to degradation by aminopeptidases or enkephalinase, a zinc metalloproteinase that cleaves a variety of bioactive peptides (*49, 50*).

Role of a Peptide Bond in the Peptide—Receptor Interactions. Functional differences between Met-enkephalin and Enk-O-Apn indicate a significant role of a peptide bond in the interactions between Met-enkephalin and opioid receptors. As shown in Table 2, the removal of a single peptide bond between otherwise flexible Gly2-Gly3 residues in Met-enkephalin resulted in a 4 orders of magnitude decrease in binding affinity, corresponding to an approximately 5.6 kcal mol^{-1} decrease in the binding energy. Our finding is in agreement with the previously described Leu-enkephalin analogue in which the amide linkages between Gly2-Gly3 were replaced by ketomethylene groups (Table 2). The authors noted that such a dramatic decrease in the affinity toward the opioid receptors was in conflict with an earlier proposed model of interactions between opioid peptides and their receptors (*51*). Our molecular modeling indicated the presence of hydrogen bonding interactions between the Gly2-Gly3 motif and several residues in δOR, including T101, D128 and Y308, suggesting that these interactions might be critical for the proper signaling of Met-enkephalin *via* δOR. Clearly more mutagenesis studies are necessary to verify this prediction.

Significance. Characterization of Met-enkephalin analogues containing backbone spacers resulted in two unexpected new findings. First, a single peptide bond between two Gly residues is a critical determinant of the interactions between opioid peptides and their receptors mediated *via* a hydrogen bonding network. The backbone spacers may therefore provide useful tools for probing interactions between ligand-binding pockets in GPCRs and their interactions with agonists

and/or antagonists. For example, ligand libraries were recently used to probe differences in the shape of the hydrophobic binding pocket in GPCRs (*52*). Furthermore, the activation of GPCRs triggers conformational rearrangements of transmembrane domains (*53*), previously described for μORs (*54*). To learn how GPCRs mediate signal transmission will require structural studies of the receptors in the free and ligand-bound states (*31, 55*), as well as a repertoire of unique, yet related, agonists and/or antagonists that differentially modulate receptor function. We trust that the enkephalin analogues containing backbone spacers will contribute to a better understanding of how the opioid receptors recognize their endogenous agonists.

Second, our results reveal a novel mechanism of seizure control in the brain that may involve interactions between opioid peptides and non-opioid receptors. Such cross-talk of neuroactive peptides and their receptors has a precedence, since dynorphin A can directly interact with bradykinin receptors in the spinal cord and mediate pronociceptive effects (*56, 57*). The resulting hyperalgesia could be reversed by selective bradykinin receptor antagonists, suggesting that this peptide-receptor cross-talk is of physiological significance. Our data suggest that opioid peptides may control seizures in the brain *via* cross-talk to non-opioid receptors; this is further illustrated in Figure 7. The endogenous Met-enkephalin can modulate both pain and seizures in the brain (indeed, there is a substantial up-regulation of enkephalin levels following seizures). Enk-O-Apn could fully suppress seizures in the brain, however, these anticonvulsant effects were not reversed by opioid antagonists. Other peptinergic systems that control seizures in the brain are apparent candidates as cross-talk partners for opioid peptides, including galanin (*44*), neurotensin (*58*), somatostatin, or NPY receptors (*59*); however, we can not exclude effects at orphan GPCRs. We hope that this work will trigger more neuropharmacological studies to dissect the mechanism of seizure control by endogenous Met-enkephalin and backbone-spacer containing analogues.

In summary, the Met-enkephalin analogues containing backbone spacers described herein provide useful lead compounds to decipher the interactions between peptinergic systems in the brain that control seizures. Our work further emphasizes the usefulness of backbone prosthesis in generating novel structural and functional properties in bioactive peptides.

METHODS

Chemical Synthesis. Peptide analogues were synthesized on amide methylbenzhydrylamine (MBHA) resin using Fmoc chemistry. For coupling of backbone spacers, the following derivatives were used: Fmoc-amino-3-oxapentanoic acid, Fmoc-aminobutyric acid, Fmoc-aminopentanoic acid, Fmoc-aminohexanoic acid, and Fmoc-aminoheptanoic acid. Peptides were purified by RP-HPLC using a semipreparative C_{18} Vydac column (218TP510) in a linear gradient (5−40%) of Buffer B (90% acetonitrile in 0.1% trifluoroacetic acid). The molecular weight of the analogues was confirmed by MALDI-TOF mass spectrometry.

Molecular Modeling. Met-enkephalin and its analogues were subjected to MD simulation using the GROMACS (v 3.3.1) package of programs (*60*). Initial coordinates for Met-enkephalin were taken from the NMR-derived structure (*61*). Backbone-spacer derivatives were built into this model using InsightII (Accelrys Inc.). MD simulations were performed using the OPLS-aa force field (*62*); amino terminus and carboxyl terminus were assumed to be in their ionized form. Each molecule was placed in a $30 \times 30 \times 30$ Å^3 water box with no pressure coupling. Met-enkephalin and water were coupled separately to a thermal bath at 300 K using a Berendsen thermostat (*63*) applied with a coupling time of 0.1 ps. All simulations were performed with a single non-bonded cutoff of 10 Å, applying a neighbor-list update frequency of 10 steps (20 fs). The particle-mesh Ewald method was used to account for long-range electrostatics, applying a grid width of 1.2 Å, and a fourth-order spline interpolation. Bond lengths were constrained using the LINCS algorithm (*64*). All simulations consisted of an initial minimization of water molecules followed by 100 ps of MD with the Met-enkephalin fixed. Following positional restraints MD, the restraints on the Met-enkephalin were removed and MD was continued for a further 100 ns. Coordinates were archived every 200 ps along the MD trajectory.

Models of δOR was constructed using the recently determined structure of the β_2 adrenergic GPCR (*55*) as a template using the MODELLER program (*65*). Complexes of Met-enkephalin with δOR were modeled using the ZDOCK program (*66*); docking was restricted to the central core of the receptor to exclude binding to the receptor exterior. One hundred models of the ligand, archived from the MD simulation, were docked to each of 25 models of the receptor. The top 2×10^3 scoring predictions from each combination were then refined using the RDOCK program (*67*). From the 5×10^6 resulting RDOCK energies, the top 100 ranking configurations were subjected to further MD refinement using the CHARMM package (*68*); high-temperature conformational sampling was achieved by initial heating and equilibration at 600 K, followed by constant temperature MD (500 ps), subsequent quenched MD, and minimization. The interaction energy between ligand and receptor was evaluated from the sum of van der Waals, electrostatic and hydrogen-bond energies.

Receptor Binding Studies. Competitive binding assays were performed on CHO (Chinese Hamster Ovary) cells expressing human δOR. Cells were plated in black costar 96-well plates at a density of 12,000 cells per well and were allowed to grow for 3 days. On the day of experiments, media was aspirated from all wells, and 50 μL of non-labeled ligand (dilutions ranging from micromolar to picomolar) and 50 μL of europium-labeled DPLCE

(10 nM) were added to each well. Ligands were diluted in binding buffer (Dulbecco's modified eagle's medium, 1 mM 1,10-phenanthroline, 200 mg L^{-1} bacitracin, 0.5 mg L^{-1} leupeptin, 0.3% BSA), and samples were prepared in quadruplicate. Cells were incubated in the presence of ligands at 37 °C and 5% CO_2 for 1.5 h. Following incubation, cells were washed 4 times with wash buffer (50 mM Tris-HCl pH 7.5, 0.2% BSA, 30 mM $MgCl_2$) using SkanWasher (Molecular Devices). Enhancement solution (Perkin-Elmer) was added (100 μL per well), and the plates were incubated at 37 °C for 30 min prior to reading. The plates were read (340 nm excitation, 400 μs decay, and emission collection at 615 nm for 400 μs) on a Wallace VICTOR^3 instrument (Perkin-Elmer). Competition curves were analyzed with GraphPad Prism using the sigmoidal dose−response (variable slope) classical equation for non-linear regression analysis. Binding assays for μOR and κOR were performed by Novascreen. For the μOR binding assay, the recombinant human receptor was expressed in CHO cells and [^{3}H]diprenorphine used as a radioligand. For the κOR binding assay, guinea pig cerebellar membranes were used as the receptor source and [^{3}H]U-69593 was used as a radioligand.

Intracellular Calcium Mobilization Assay. This functional assay was performed by Multispan, Inc. HEK-293T cells transiently co-transfected with chimeric Gα and either δOR or μOR were plated in 96-well plates and grown to confluence. After 30 min of incubation with Fluo-3/Am, cells were washed with HBS buffer (10 mM HEPES, 150 mM NaCl, 3 mM EDTA, pH 7.4) and equilibrated for an additional 30 min. The fluorescence emission due to intracellular calcium mobilization elicited by agonists of the expressed receptor was determined with a fluorescence imaging plate reader (FLIPR, Molecular Devices Corporation). The results were analyzed using SOFTmax Pro and GraphPad Prism.

Anticonvulsant Activity. Analogues were tested in the 6 Hz partial psychomotor seizure model (6 Hz, 32 mA, 3 s) following icv administration to adult male CF-1 mice (Charles River). The TPE for each of the Met-enkephalin analogues was determined to be 30 min. Next, at the TPE (30 min), rotorod performance was evaluated. Under normal conditions, mice treated with vehicle can remain indefinitely on a rotorod rotating at 6 rpm. If a treated mouse fell off the rotorod more than 3 times in a 1 min observation period, the analogue was considered to have adversely affected rotorod performance. Immediately after the completion of the rotorod test (at each dose), individual mice were tested in the 6 Hz seizure model. Increasing doses of each analogue were evaluated in order to determine their dose−response. A minimum of four concentrations of each analogue were tested unless the behavioral side effects observed in the rotorod test precluded testing at higher concentrations. Mice were considered protected if they did not display motor seizure activity characterized by vibrissae twitching, jaw chomping, or forelimb clonus. For each dose, eight mice were used. For each analogue where a dose−response could be determined, ED_{50} values were calculated using Probit analysis software (*69*). For the reversal experiments with naloxone, mice were pretreated with 5 mg kg^{-1} naloxone or 0.9% saline (ip). At the TPE of naloxone (30 min), mice received either Met-enkephalin or Enk-O-Apn (2 nmol, 5 μL, icv). Thirty minutes later, mice were challenged with corneal stimulation (6 Hz, 32 mA, 3 s). For the reversal experiment with naloxonazine, mice were dosed with 35 mg kg^{-1} of naloxonazine or saline (sc). At the TPE of naloxonazine (24 h), mice were dosed with either Met-enkephalin or Enk-O-Apn. Thirty minutes later, mice were challenged with corneal stimulation. For the statistical analysis, we employed non-parametric statistics to assess whether the number of mice protected in the 6 Hz tests was significantly different in saline-treated mice versus those which were treated with either naloxone or naloxonazine. Since no statistical difference was found between two saline-treated groups in the two independent studies, these results were pooled to give a total $n = 16$ animals. The results were then compared *via* one-way ANOVA with non-parametric statistics (Kruskal−Wallis test). GraphPad Prism was employed to evaluate a Dunn's posthoc analysis of the comparisons to identify statistically significant differences ($p < 0.05$). However, since no significant differences were detected, no posthoc comparisons were reported. No significant difference between the anticonvulsant results or the toxicity data were observed between saline/analogue-treated group and antagonist/analogue-treated group. All animal procedures were carried out according to the protocol approved by the IUCAC Committee at the University of Utah.

Antinociceptive Assay. The effect of each test peptide on pain sensitivity was determined in the formalin-induced licking test. For this test, a mouse (25−30 g) was placed in an individual open plexiglass cylinder (4 in. diameter, 8 in. height). Prior to the injection of formalin, a test peptide or vehicle (0.9% saline) was administered to the individual mouse (icv). At the TPE of each analogue (15 min), formalin was injected into the ipsilateral paw *via* intraplantar injection (5% formalin, 10 μL). Mice (two at a time) were observed for 45 min, and the paw-licking time was determined for the first 2 min of every 5 min interval. The behavioral outcome of the formalin assay was characterized by a biphasic response where the phase I (acute) of the licking response was quantified within the first 10 min and the phase II (inflammatory) response is quantified between 10−40 min. The area under the curve (AUC) for each phase was calculated, and the results were compared to the AUCs for each phase of the saline-treated group. For each dose, eight mice were used. Using GraphPad Prism, the average percentage for both the analogue-treated group and the saline-treated group were calculated, and then tested for significant differences *via* unpaired *t* test. Results were considered significantly different from saline-treated group if the *p*-value was <0.05. When statistical significance was detected, the *p*-values were reported. For the reversal experiment with naloxone, mice were dosed with 5 mg kg^{-1} of naloxone or saline (ip). At the TPE of naloxone (30 min), a test peptide or vehicle was administered to the individual mouse (icv). Fifteen minutes later, formalin was injected into the ipsilateral paw *via* intraplantar injection. Mice (two at a time) were observed for 45 min. For the reversal experiment with naloxonazine, mice were dosed with 35 mg kg^{-1} of naloxonazine or saline (sc). At the TPE of naloxonazine (24 h), a test peptide or vehicle was administered to the individual mouse (icv). Fifteen minutes later, formalin was injected into the ipsilateral paw *via* intraplantar injection. Mice (two at a time) were observed for 45 min.

Metabolic Stability. The stability of the analogues in 20% rat serum was measured at 37 °C. Triplicate samples were assayed at a concentration of 0.25 μg μL^{-1}. At 0, 5, 15, 30, 60, and 120 min, 200 μL of the reaction mixture was removed and added to 100 μL of TCA mix (15% trichloroacetic acid, 40% isopropanol) to precipitate serum proteins. After 15 min of incubation at −20 °C, the precipitate was spun down, and the supernatant was analyzed by RP-HPLC. Aliquots of the samples were injected, and the amount of remaining intact analogue was determined by integration of the RP-HPLC peaks recovered at 210 nm.

Acknowledgment: This work was supported by a start-up fund from the University of Utah, Department of Medicinal Chemistry. G.B. also acknowledges financial support from the National Institutes of Health grants NS059669 and GM 48677. R.J.G. acknowledges a financial support from the National Institutes of Health (R01-CA097360). B.J.S. acknowledges the NHMRC and Victorian State government for infrastructure support through the IRIIS (361646) and OIS grants. We would like to thank L. Zhang and B. R. Green for their assistance with pep-

tide synthesis. G.B. and H.S.W. are scientific cofounders of NeuroAdjuvants, Inc.

Supporting Information Available: This material is available free of charge *via* the Internet at http://pubs.acs.org.

REFERENCES

1. Vagner, J., Qu, H., and Hruby, V. J. (2008) Peptidomimetics, a synthetic tool of drug discovery, *Curr. Opin. Chem. Biol. 12*, 292–296.
2. Goodman, C. M., Choi, S., Shandler, S., and Degrado, W. F. (2007) Foldamers as versatile frameworks for the design and evolution of function, *Nat. Chem. Biol. 3*, 252–262.
3. Anderson, G. J. (1997) Incorporation of stable pseudopeptide bonds. Methylene amino, thioether, and hydroxyethylene derivatives, *Methods Mol. Biol. 73*, 49–60.
4. Arnold, U., Hinderaker, M. P., Nilsson, B. L., Huck, B. R., Gellman, S. H., and Raines, R. T. (2002) Protein prosthesis: a semisynthetic enzyme with a β-peptide reverse turn, *J. Am. Chem. Soc. 124*, 8522–8523.
5. Arnold, U., Hinderaker, M. P., Köditz, J., Golbik, R., Ulbrich-Hofmann, R., and Raines, R. T. (2003) Protein prosthesis: a nonnatural residue accelerates folding and increases stability, *J. Am. Chem. Soc. 125*, 7500–7501.
6. Chatterjee, S., Roy, R. S., and Balaram, P. (2007) Expanding the polypeptide backbone: qhdrogen-bonded conformations in hybrid polypeptides containing the higher homologues of α-amino acids, *J. R. Soc. Interface 4*, 587–606.
7. Biron, E., Chatterjee, J., Ovadia, O., Langenegger, D., Brueggen, J., Hoyer, D., Schmid, H. A., Jelinek, R., Gilon, C., Hoffman, A., and Kessler, H. (2008) Improving oral bioavailability of peptides by multiple N-methylation: somatostatin analogues, *Angew. Chem., Int. Ed. 47*, 2595–2599.
8. Green, B. R., Catlin, P., Zhang, M.-M., Fiedler, B., Bayudan, W., Morrison, A., Norton, R. S., Smith, B. J., Yoshikami, D., Olivera, B. M., and Bulaj, G. (2007) Conotoxins containing nonnatural backbone spacers: cladistic-based design, chemical synthesis, and improved analgesic activity, *Chem. Biol. 14*, 399–407.
9. Rist, B., Wieland, H. A., Willim, K. D., and Beck-Sickinger, A. G. (1995) A rational approach for the development of reduced-size analogues of neuropeptide Y with high affinity to the Y1 receptor, *J. Pept. Sci. 1*, 341–348.
10. Koskinen, A. M. P., Valo, T., Vihavainen, S., and Hakala, J. M. L. (1995) Synthesis of α-helix substituted analogs of calcitonin gene-related peptide, *Bioorg. Med. Chem. Lett. 5*, 573–578.
11. Trauger, J. W., Kohli, R. M., and Walsh, C. T. (2001) Cyclization of backbone-substituted peptides catalyzed by the thioesterase domain from the tyrocidine nonribosomal peptide synthetase, *Biochemistry 40*, 7092–7098.
12. Doyle, M. E., Greig, N. H., Holloway, H. W., Betkey, J. A., Bernier, M., and Egan, J. M. (2001) Insertion of an N-terminal 6-aminohexanoic acid after the 7 amino acid position of glucagon-like peptide-1 produces a long-acting hypoglycemic agent, *Endocrinology 142*, 4462–4468.
13. Hruby, V. J., and Agnes, R. S. (1999) Conformation-activity relationships of opioid peptides with selective activities at opioid receptors, *Biopolymers 51*, 391–410.
14. Janecka, A., Fichna, J., and Janecki, T. (2004) Opioid receptors and their ligands, *Curr. Top. Med. Chem. 4*, 1–17.
15. Polt, R., Dhanasekaran, M., and Keyari, C. M. (2005) Glycosylated neuropeptides: a new vista for neuropsychopharmacology? *Med. Res. Rev. 25*, 557–585.
16. Schiller, P. W. (2005) Opioid peptide-derived analgesics, *AAPS J. 7*, E560–E565.
17. Mosberg, H. I., Hurst, R., Hruby, V. J., Gee, K., Yamamura, H. I., Galligan, J. J., and Burks, T. F. (1983) Bis-penicillamine enkephalins possess highly improved specificity toward δ opioid receptors, *Proc. Natl. Acad. Sci. U.S.A. 80*, 5871–5874.
18. Bartosz-Bechowski, H., Davis, P., Zalewska, T., Slaninova, J., Porreca, F., Yamamura, H. I., and Hruby, V. J. (1994) Cyclic enkephalin analogs with exceptional potency at peripheral delta opioid receptors, *J. Med. Chem. 37*, 146–150.
19. Elmagbari, N. O., Egleton, R. D., Palian, M. M., Lowery, J. J., Schmid, W. R., Davis, P., Navratilova, E., Dhanasekaran, M., Keyar, C. M., Yamamura, H. I., Porreca, F., Hruby, V. J., Polt, R., and Bilsky, E. J. (2004) Antinociceptive structure-activity studies with enkephalin-based opioid glycopeptides, *J. Pharmacol. Exp. Ther. 311*, 290–297.
20. Egleton, R. D., Mitchell, S. A., Huber, J. D., Palian, M. M., Polt, R., and Davis, T. P. (2001) Improved blood-brain barrier penetration and enhanced analgesia of an opioid peptide by glycosylation, *J. Pharmacol. Exp. Ther. 299*, 967–972.
21. Egleton, R. D., Mitchell, S. A., Huber, J. D., Janders, J., Stropova, D., Polt, R., Yamamura, H. I., Hruby, V. J., and Davis, T. P. (2000) Improved bioavailability to the brain of glycosylated Met-enkephalin analogs, *Brain Res. 881*, 37–46.
22. Bilsky, E. J., Egleton, R. D., Mitchell, S. A., Palian, M. M., Davis, P., Huber, J. D., Jones, H., Yamamura, H. I., Janders, J., Davis, T. P., Porreca, F., Hruby, V. J., and Polt, R. (2000) Enkephalin glycopeptide analogues produce analgesia with reduced dependence liability, *J. Med. Chem. 43*, 2586–2590.
23. Chandrakumar, N. S., Stapelfeld, A., Beardsley, P. M., Lopez, O. T., Drury, B., Anthony, E., Savage, M. A., Williamson, L. N., and Reichman, M. (1992) Analogs of the δ opioid receptor selective cyclic peptide [2-D-penicillamine,5-D-penicillamine]-enkephalin: 2′,6′-dimethyltyrosine and Gly3-Phe4 amide bond isostere substitutions, *J. Med. Chem. 35*, 2928–2938.
24. Gupta, G., Sarma, M. H., Sarma, R. H., and Dhingra, M. M. (1986) NOE data at 500 MHz reveal the proximity of phenyl and tyrosine rings in enkephalin, *FEBS Lett. 198*, 245–250.
25. van der Spoel, D., and Berendsen, H. J. (1997) Molecular dynamics of Leu-enkephalin in water and DMSO, *Biophys. J. 72*, 2032–2041.
26. Handl, H. L., Vagner, J., Yamamura, H. I., Hruby, V. J., and Gillies, R. J. (2005) Development of a lanthanide-based assay for detection of receptor-ligand interactions at the δ-opioid receptor, *Anal. Biochem. 343*, 299–307.
27. Loacker, S., Sayyah, M., Wittmann, W., Herzog, H., and Schwarzer, C. (2007) Endogenous dynorphin in epileptogenesis and epilepsy: anticonvulsant net effect via κ opioid receptors, *Brain 130*, 1017–1028.
28. Almquist, R. G., Olsen, C. M., Uyeno, E. T., and Toll, L. (1984) Replacement of the peptide-backbone amides connecting Tyr-Gly and Gly-Gly in leucine-enkephalin with ketomethylene groups: synthesis and biological activity, *J. Med. Chem. 27*, 115–120.
29. Harrison, B. A., Gierasch, T. M., Neilan, C., Pasternak, G. W., and Verdine, G. L. (2002) High-affinity mu opioid receptor ligands discovered by the screening of an exhaustively stereodiversified library of 1,5-enediols, *J. Am. Chem. Soc. 124*, 13352–13353.
30. Snyder, K. R., Murray, T. F., DeLander, G. E., and Aldrich, J. V. (1993) Synthesis and opioid activity of dynorphin A-(1-13)NH_2 analogues containing *cis*- and *trans*-4-aminocyclohexanecarboxylic acid, *J. Med. Chem. 36*, 1100–1103.
31. Jaakola, V. P., Griffith, M. T., Hanson, M. A., Cherezov, V., Chien, E. Y., Lane, J. R., Ijzerman, A. P., and Stevens, R. C. (2008) The 2.6 Å crystal structure of a human A_{2A} adenosine receptor bound to an antagonist, *Science 322*, 1211–1217.
32. Décaillot, F. M., Befort, K., Filliol, D., Yue, S. Y., Walker, P., and Kieffer, B. L. (2003) Opioid receptor random mutagenesis reveals a mechanism for G protein-coupled receptor activation, *Nat. Struct. Biol. 10*, 629–636.
33. Valiquette, M., Vu, H. K., Yue, S. Y., Wahlestedt, C., and Walker, P. (1996) Involvement of Trp-284, Val-296 and Val-297 of the human δ-opioid receptor in binding of δ-selective ligands, *J. Biol. Chem. 271*, 18789–18796.

34. Befort, K., Tabbara, L., Kling, D., Maigret, B., and Kieffer, B. L. (1996) Role of aromatic transmembrane residues of the δ-opioid receptor in ligand recognition, *J. Biol. Chem. 271*, 10161–10168.
35. Pogozheva, I. D., Lomize, A. L., and Mosberg, H. I. (1998) Opioid receptor three-dimensional structures from distance geometry calculations with hydrogen bonding constraints, *Biophys. J. 75*, 612–634.
36. Aburi, M., and Smith, P. E. (2004) Modeling and simulation of the human δ opioid receptor, *Protein Sci. 13*, 1997–2008.
37. Lapalu, S., Moisand, C., Mazarguil, H., Cambois, G., Mollereau, C., and Meunier, J.-C. (1997) Comparison of the structure-activity relationships of nociceptin and dynorphin A using chimeric peptides, *FEBS Lett. 417*, 333–336.
38. Schlechtingen, G., DeHaven, R. N., Daubert, J. D., Cassel, J. A., Chung, N. N., Schiller, P. W., Taulane, J. P., and Goodman, M. (2003) Structure-activity relationships of dynorphin a analogues modified in the address sequence, *J. Med. Chem. 46*, 2104–2109.
39. Morris, B. J., and Johnston, H. M. (1995) A role for hippocampal opioids in long-term functional plasticity, *Trends Neurosci. 18*, 350–355.
40. Koide, S., Onishi, H., Katayama, M., and Yamagami, S. (1993) Endogenous methionine enkephalin may play an anticonvulsant role in the seizure-susceptible El mouse, *Neurochem. Res. 18*, 1259–1262.
41. Tortella, F. C., Robles, L., and Mosberg, H. I. (1987) Evidence for *mu* opioid receptor mediation of enkephalin-induced electroencephalographic seizures, *J. Pharmacol. Exp. Ther. 240*, 571–577.
42. Barton, M. E., Peters, S. C., and Shannon, H. E. (2003) Comparison of the effect of glutamate receptor modulators in the 6 Hz and maximal electroshock seizure models, *Epilepsy Res. 56*, 17–26.
43. Kaminski, R. M., Livingood, M. R., and Rogawski, M. A. (2004) Allopregnanolone analogs that positively modulate $GABA_A$ receptors protect against partial seizures induced by 6-Hz electrical stimulation in mice, *Epilepsia 45*, 864–867.
44. Bulaj, G., Green, B. R., Lee, H., Robertson, C. R., White, K., Zhang, L., Sochanska, M., Flynn, S. P., Scholl, E. A., Pruess, T. H., Smith, M. D., and White, H. S. (2008) Design, synthesis, and characterization of high-affinity, systemically-active galanin analogues with potent anticonvulsant activities, *J. Med. Chem. 51*, 8038–8047.
45. Barton, M. E., Klein, B. D., Wolf, H. H., and White, H. S. (2001) Pharmacological characterization of the 6 Hz psychomotor seizure model of partial epilepsy, *Epilepsy Res. 47*, 217–227.
46. Smith, M. D., Wilcox, K. S., and White, H. S. (2007) Discovery of antiepileptic drugs, *Neurotherapeutics 4*, 12–17.
47. Nakamura, M., and Ferreira, S. H. (1988) Peripheral analgesic action of clonidine: mediation by release of endogenous enkephalin-like substances, *Eur. J. Pharmacol. 146*, 223–228.
48. Hurley, R. W., and Hammond, D. L. (2001) Contribution of endogenous enkephalins to the enhanced analgesic effects of supraspinal μ opioid receptor agonists after inflammatory Injury, *J. Neurosci. 21*, 2536–2545.
49. Matsas, R., Kenny, A. J., and Turner, A. J. (1984) The metabolism of neuropeptides. The hydrolysis of peptides, including enkephalins, tachykinins and their analogues, by endopeptidase-24.11, *Biochem. J. 223*, 433–440.
50. Roques, B. P., Noble, F., Daugé, V., Fournié-Zaluski, M.-C., and Beaumont, A. (1993) Neutral endopeptidase 24.11: structure, inhibition, and experimental and clinical pharmacology, *Pharmacol. Rev. 45*, 87–146.
51. Hudson, D., Sharpe, R., and Szelke, M. (1980) Methionine enkephalin and isosteric analogues. Part II: receptor conformation of methionine enkephalin, *Int. J. Peptide Protein Res. 15*, 122–129.
52. Schürer, S. C., Brown, S. J., Gonzalez-Cabrera, P. J., Schaeffer, M. T., Chapman, J., Jo, E., Chase, P., Spicer, T., Hodder, P., and Rosen, H. (2008) Ligand-binding pocket shape differences between sphingosine 1-phosphate (S1P) receptors S1P1 and S1P3 determine efficiency of chemical probe identification by ultrahigh-throughput screening, *ACS Chem. Biol. 3*, 486–498.
53. Park, P. S., Lodowski, D. T., and Palczewski, K. (2008) Activation of G protein-coupled receptors: beyond two-state models and tertiary conformational changes, *Annu. Rev. Pharmacol. Toxicol. 48*, 107–141.
54. Xu, W., Sanz, A., Pardo, L., and Liu-Chen, L. (2008) Activation of the μ opioid receptor involves conformational rearrangements of multiple transmembrane domains, *Biochemistry 47*, 10576–10586.
55. Cherezov, V., Rosenbaum, D. M., Hanson, M. A., Rasmussen, S. G., Thian, F. S., Kobilka, T. S., Choi, H. J., Kuhn, P., Weis, W. I., Kobilka, B. K., and Stevens, R. C. (2007) High-resolution crystal structure of an engineered human β_2-adrenergic G protein-coupled receptor, *Science 318*, 1258–1265.
56. Lai, J., Luo, M. C., Chen, Q., Ma, S., Gardell, L. R., Ossipov, M. H., and Porreca, F. (2006) Dynorphin A activates bradykinin receptors to maintain neuropathic pain, *Nat. Neurosci. 9*, 1534–1540.
57. Lai, J., Luo, M. C., Chen, Q., and Porreca, F. (2008) Pronociceptive actions of dynorphin via bradykinin receptors, *Neurosci. Lett. 437*, 175–179.
58. Lee, H., Zhang, L., Smith, M. D., White, H. S., and Bulaj, G. (2009) Glycosylated neurotensin analogues exhibit sub-picomolar anticonvulsant potency in a pharmacoresistant model of epilepsy, *ChemMedChem 3*, 400–405.
59. Brumovsky, P., Shi, T. S., Landry, M., Villar, M. J., and Hökfelt, T. (2007) Neuropeptide tyrosine and pain, *Trends Pharmacol. Sci. 93*–102.
60. Lindahl, E., Hess, B., and van der Spoel, D. (2001) GROMACS 3.0: A package for molecular stimulation and trajectory analysis, *J. Mol. Mod. 7*, 306–317.
61. Marcotte, I., Separovic, F., Auger, M., and Gagné, S. M. (2004) A multidimensional ^{1}H NMR investigation of the conformation of methionine-enkephalin in fast-tumbling micelles, *Biophys. J. 86*, 1587–1600.
62. Jorgensen, W. L., and Tirado-Rives, J. (1988) The OPLS potential functions for proteins. Energy minimizations for crystals of cyclic peptides of crambin, *J. Am. Chem. Soc. 110*, 1657–1666.
63. Berendsen, H. J. C., Postma, J. P. M., van Gunsteren, W. F., DiNola, A., and Haak, J. R. (1984) Molecular dynamics with coupling to an external bath, *J. Chem. Phys. 81*, 3684–3690.
64. Hess, B., Bekker, H., Berendsen, H. J. C., and Fraaije, J. G. E. M. (1977) LINCS: a linear constraint solver for molecular simulations, *J. Comput. Chem. 18*, 1463–1472.
65. Fiser, A., and Sali, A. (2003) Modeller: generation and refinement of homology-based protein structure models, *Methods Enzymol. 374*, 461–469.
66. Chen, R., Li, L., and Weng, Z. (2003) ZDOCK: an initial-stage protein-docking algorithm, *Proteins 52*, 80–87.
67. Li, L., Chen, R., and Weng, Z. (2003) RDOCK: refinement of rigid-body protein docking predictions, *Proteins 53*, 693–707.
68. MacKerell, A. D., Jr., Brooks, B., Brooks, C. L., III, Nilsson, L., Roux, B., Won, Y., and Karplus, M. (1998) CHARMM: The energy function and its parameterization with an overview of the program, in *The Encyclopedia of Computational Chemistry* (Schleyer, P. v. R., Allinger, N. L., Clark, T., Gasteiger, J., Kollman, P. A., Schaefer, H. F., III, and Schreiner, P. R., Eds.) pp 271–277, John Wiley & Sons, Chichester.
69. Finney, D. J. (1971) *Probit Analysis*, 3rd ed., Cambridge University Press, London.